5. N. E. Graham *et al.*, *J. Geophys. Res.* **92**, 14251 (1987); N. E. Graham *et al.*, *ibid.*, p. 14271.
6. T. P. Barnett and R. Preisendorfer, *Mon. Weather Rev.* **115**, 1825 (1987).
7. A. J. Busalacchi and J. J. O'Brien, *J. Geophys. Res.* **86**, 10901 (1981); *J. Phys. Oceanogr.* **10**, 1929 (1980).
8. M. Inoue *et al.*, *J. Geophys. Res.* **92**, 11671 (1987); A. J. Busalacchi and M. A. Cane, *J. Phys. Oceanogr.* **15**, 213 (1985).
9. S. E. Zebiak and M. A. Cane, *Mon. Weather Rev.* **115**, 2262 (1987).
10. S. E. Zebiak, *ibid.* **114**, 1263 (1986).
11. Both M2 and M3 use the wind analyses produced at Florida State University.
12. T. P. Barnett, *J. Phys. Oceanogr.* **11**, 1043 (1981); ——— and J. Hasselmann, *Rev. Geophys. Space Phys.* **17**, 949 (1979).
13. This appears different from the forecast given in Cane *et al.* (*4*), where the magnitude exceeds the observed. The discrepancy is partly due to the difference in lead times, but is mostly attributable to the fact that the results shown here have been scaled so that the models forecast from the period from 1970–85 match the observed mean and variance.
14. The model is initialized using only wind data and so can be verified against SST observations at the time t_0.
15. Persistence forecasts of this lead time are very poor and offer no competition for M1 and M3.
16. In fact, M3 solutions will, over a matter of years, follow fairly self-similar orbits in phase space just like the actual ENSO signal.
17. W. B. White *et al.*, *J. Phys. Oceanogr.* **15**, 386 (1985); W. B. White *et al.*, *ibid.*, p. 917.
18. T. P. Barnett, *J. Atmos. Sci.* **42**, 478 (1985).
19. Models M1A and M2 also rely only on changes in the tropical Pacific for their predictive skill.
20. P. S. Schopf and M. J. Suarez, *J. Atmos. Sci.* **45**, 549 (1988); N. E. Graham and W. B. White, *Science* **240**, 1293 (1988).
21. The authors are grateful to two anonymous reviewers whose comments were helpful in improving the original draft of this paper. This work was supported by NSF grant ATM85-13713, NOAA (TOGA) grant NA85AA-D-AC132, and the NOAA Experimental Climate Forecast Center grant NA86-AA-D-CP104 to the Scripps Institution of Oceanography; by NOAA (TOGA) grant NA87-AA-D-AC081 to Lamont-Doherty Geological Observatory; and by NSF grant OCE84-15986 to Florida State University. The support of the U.S. TOGA Project Office and the Experiment Climate Prediction Program were essential to the cooperative nature of this work.

1 February 1988; accepted 18 May 1988

Irregular Recurrence of Large Earthquakes Along the San Andreas Fault: Evidence from Trees

GORDON C. JACOBY, JR., PAUL R. SHEPPARD, KERRY E. SIEH

Old trees growing along the San Andreas fault near Wrightwood, California, record in their annual ring-width patterns the effects of a major earthquake in the fall or winter of 1812 to 1813. Paleoseismic data and historical information indicate that this event was the "San Juan Capistrano" earthquake of 8 December 1812, with a magnitude of 7.5. The discovery that at least 12 kilometers of the Mojave segment of the San Andreas fault ruptured in 1812, only 44 years before the great January 1857 rupture, demonstrates that intervals between large earthquakes on this part of the fault are highly variable. This variability increases the uncertainty of forecasting destructive earthquakes on the basis of past behavior and accentuates the need for a more fundamental knowledge of San Andreas fault dynamics.

LARGE EARTHQUAKES OCCUR ALONG the San Andreas fault northeast of Los Angeles about every 131 years (*1–4*). Unfortunately, error inherent in standard radiocarbon measurements limits resolution of individual intervals between earthquakes to about ±100% of the average interval. This imprecision hampers assessment of the annual probability of a large earthquake on the San Andreas fault in southern California. If, for example, intervals vary from the mean by no more than 10%, then the chance of such an event within the next 30 years—131 to 161 years since the great 1857 earthquake—is almost 100%. If, on the other hand, intervals vary from 50 to 300 years (*2*), then forecasting major earthquakes on the basis of average intervals is less reliable. Such variability would also nurture doubts about hypotheses of uniform fault strain accumulation and relief.

On the basis of historical information and new, high-precision radiocarbon measurements, the latest three large earthquakes on the San Andreas fault near Los Angeles occurred in A.D. 1857, 1785 ± 32, and 1480 ± 15 (*4*). The two most recent events occurred during the lifetime of many trees growing along the fault. We examined growth rings of these trees to date precisely the second most recent event and to estimate its fault rupture length.

That trees are affected by large earthquakes is well known (*5*). Tree damage is even a criterion for assigning shaking intensities of VIII and above on the modified Mercalli intensity scale (MMI) (*6*). Such high intensities are typically limited to within a few kilometers of the seismic source, that is, the earthquake fault. Earlier investigators have successfully used trees to study earthquakes (*7, 8*), and a detailed review of dendroseismologic studies is in Sheppard and Jacoby (*9*).

The 1857 San Andreas rupture segment traverses three forested areas (Fig. 1); we reconnoitered each for old trees. The southernmost area, in and northwest of Wrightwood, contained the most promising trees. Sixty-five old Jeffrey pines (*Pinus jeffreyi* Grev. and Balf.), two white firs [*Abies concolor* (Gord. and Glend.) Lindl. ex Hildebt.], and three incense-cedars [*Libocedrus decurrens* (Torr.) Florin.] growing either in or around the fault zone were cored at breast-height with 5-mm-diameter corers. Cross sections were also collected from several stumps.

Using standard dendrochronological techniques (*10*), we cross-dated all cores and sections both within and between trees and with the Mill Creek Summit chronology (*11*), a tree-ring index series developed from nearby big-cone Douglas-fir [*Pseudotsuga macrocarpa* (Vassey) Mayr] (Fig. 1). We cross-dated each core by locating particularly narrow rings produced during droughts in 1782, 1795, 1809, 1813, 1823, 1841, 1843, 1845, 1857, and 1864. We then measured all ring widths to the nearest 0.01 mm with a computerized dendrometer (*12*). Missing rings were evident in some cores and were assigned widths of zero following dendrochronological procedures (*10*). Consecutive missing rings were evident in two trees that lost most of their crowns at some point in time. The most probable time for trees to cease radial growth is just after severe trauma, such as major crown loss (*13*). Hence, zeros were assigned for those missing rings immediately following the onset of trauma.

We combined measured ring-width series from trees growing away from the fault zone in a single control chronology for the period A.D. 1600 to 1900 by the use of autoregressive standardization (*14*) (Fig. 2, uppermost plot). This chronology corresponds well with other tree-ring chronologies from throughout southern California (*11*); only regional phenomena (typically climatic fluctuation) produce variations in control chronologies.

Nine conifers sampled in the Wrightwood area suffered unusual trauma, as indicated by suppressed ring growth, beginning in 1813 (Fig. 2). In all but one of these trees, this suppression was the greatest growth anomaly during their life-spans (*15*). Four trees (Pool Tree, Lone Pine Canyon, Wrightwood 3-1, and Wrightwood 3-2)

G. C. Jacoby, Jr., and P. R. Sheppard, Tree-Ring Laboratory, Lamont-Doherty Geological Observatory, Palisades, NY 10964.
K. E. Sieh, Division of Geological and Planetary Sciences, California Institute of Technology, Pasadena, CA 91125.

took more than half a century to recover. Pool Tree and Lone Pine Canyon (the two that lost their crowns) show the most severe growth suppression. Wrightwood 3-2 also lost some of its crown, but not as much as the other two.

The other disturbed trees indicate trauma as several years of suppressed growth beginning in 1813 (Fig. 2). The Wrightwood chronology shows that trees in the area experienced reduced growth in 1813, probably because of regional drought. During the remainder of the decade, however, most trees produced normally varying ring widths. In contrast, the disturbed trees continued to form narrow rings for several years after 1813. Such prolonged suppression cannot be attributed to drought, which causes acute, diminished ring growth for single years. For example, Pool Tree and Lone Pine Canyon have no missing rings from 1700 to 1812 even though severe droughts occurred in 1707, the 1730s, 1754, 1765, 1777, 1782, 1795, and 1809.

The nine trees were disturbed between September 1812 and April 1813. The last cells that formed during the 1812 growing season appear healthy, indicating that the trauma occurred after the growing season. Jeffrey pines in this region typically end seasonal growth in September with the formation of thick-walled, radially flattened latewood cells. In this respect, the disturbed trees are similar to the undisturbed trees for 1812. If the disturbance occurred before the season's end, then fewer rows of latewood cells would have formed in the disturbed trees. The absence of robust 1813 earlywood cells in the traumatized trees indicates that they were disturbed before the onset of 1813 growth. Because radial cell division in Jeffrey pine usually starts in late March (*16*), we conclude that the disturbance occurred before April 1813.

All nine disturbed trees are within 20 m of the San Andreas fault, and they extend along 12 km of fault (Fig. 1, inset). This spatial distribution indicates that slip along the San Andreas fault effected the trauma. Neither lightning, severe wind, ice storm, fire, disease, nor insect infestation can produce trauma that is synchronous and linearly restricted. Even severe seismic shaking can be ruled out because it also would have damaged trees outside the fault zone. A plausible cause of physical damage to the nine trees is severance of major roots during right-lateral slip and warping along the fault. Loss of major roots could greatly diminish nutrient and water uptake for decades until new roots regenerated. Branch loss or crown topping resulting from sudden fault slippage could have a similar effect.

The event recorded by our nine trees is probably associated with one of the three large southern California earthquakes of December 1812 (*17*). One occurred on 8 December and was reported from San Diego to the Santa Barbara region (Fig. 1). The other two occurred on 21 December and were felt most severely near Santa Barbara (*18*). These three quakes were previously ascribed to coastal or near-coastal faults because of damage reported in coastal communities (*17*).

For the two 21 December shocks, a coastal source near Santa Barbara is certain; numerous aftershocks were felt locally and several odd disturbances of the sea were reported (*17*). On the basis of regional historical records, shaking intensities (MMI) near Santa Barbara were estimated at about VIII and magnitudes (M_W) at about 7.1. The San Andreas fault is not a plausible source for the 21 December quakes because even the great (M_W = 7.9) 1857 earthquake, which involved slip on the San Andreas fault at its closest point to Santa Barbara, was not as intense in Santa Barbara as were these events (*3*).

Although reports of shaking on 8 December 1812 are incomplete and ambiguous, they allow an interpretation that the San Andreas fault was that earthquake's source. As in the great 1857 earthquake, low to moderate levels of shaking (without serious damage) were reported in the San Diego and Santa Barbara regions (*17*) (Fig. 1). High intensity (MMI = VII) shaking was felt on 8 December 1812 at San Buenaventura, San Fernando, and San Gabriel, which reported the most extensive damage. The similarity of intensities at these locations for both 1812 and 1857 suggests that a major part of the San Andreas fault near Los Angeles ruptured on 8 December 1812.

Two arguments against a source on the San Andreas fault for the 8 December quake are that a new church at San Juan Capistrano was severely damaged and that there are no reports of damage for settlements east of San Gabriel, which are nearer to the fault than the coastal communities. Neither argument, however, is convincing in conjunction with other information. The severe damage of the church has been reasonably attributed to poor construction, which commenced in 1797 with neophytes and padres (*18, 19*). The stone mason–architect did not arrive until 1799, and he subsequently died in 1803; the church was finished without him (*19*). Furthermore, although this new church was irreparably damaged, an adja-

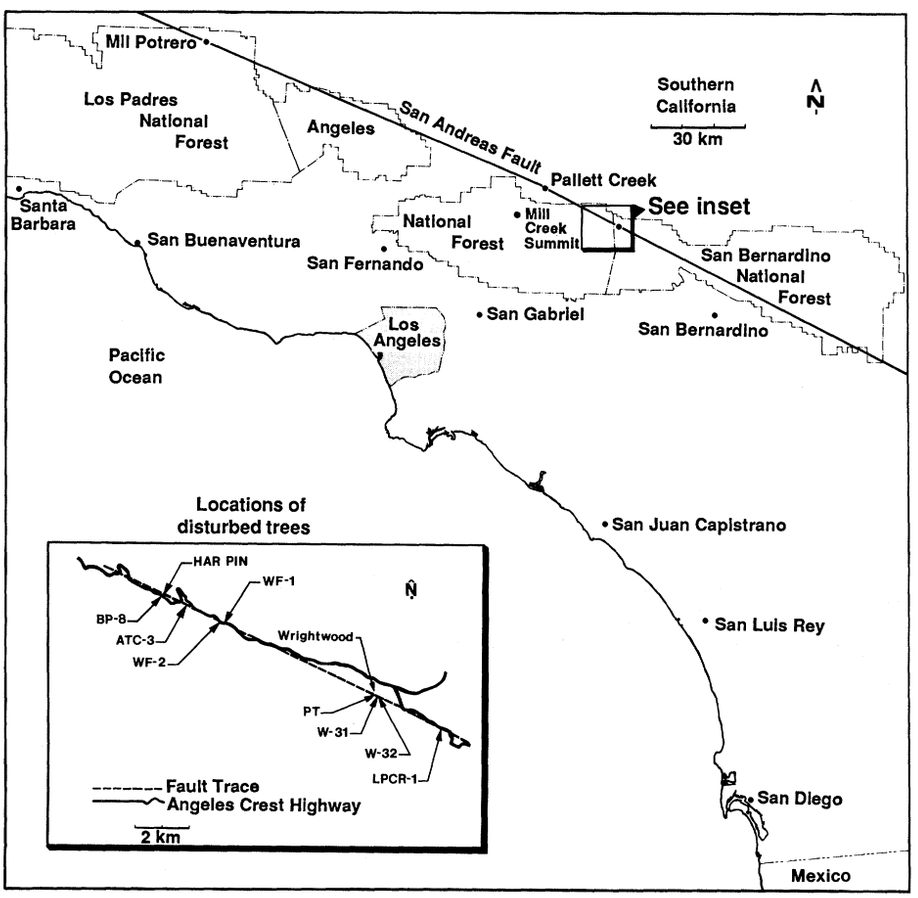

Fig. 1. Map of study area. Inset shows locations of disturbed trees (abbreviations given in Fig. 2). Trees in the same vicinity but at greater distances from the fault are undisturbed.

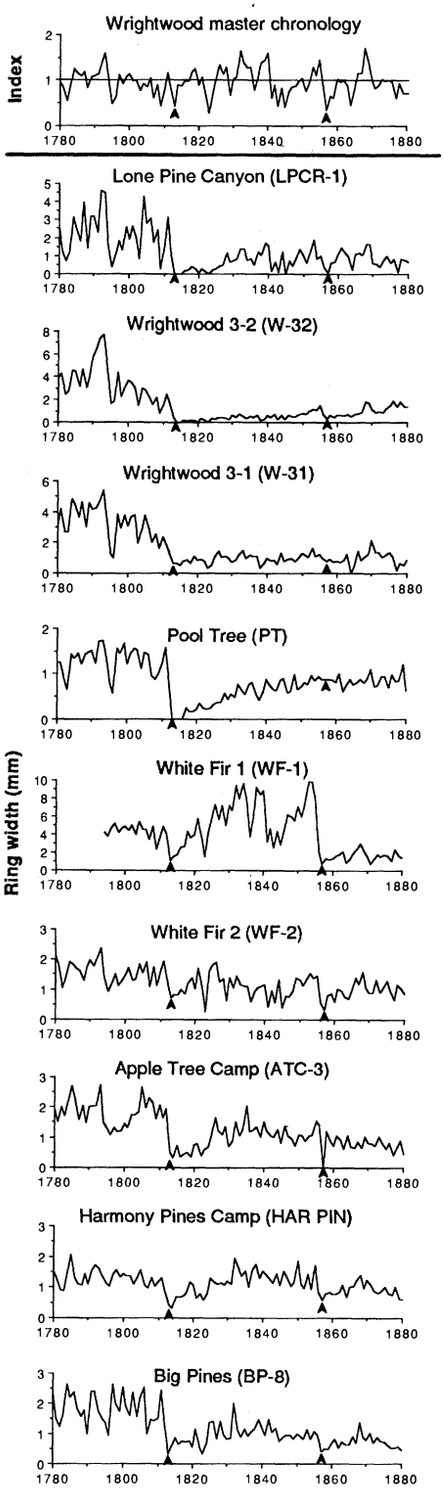

Fig. 2. Time series plots (from 1780 to 1880) of standardized ring-width indices from the Wrightwood master chronology (undisturbed) and of ring widths of one radius from each disturbed tree. Arrowheads point to 1813 and 1857. The low indices in the master chronology correspond to the drought years mentioned in the text. Trees in the master chronology recover in 1814 from the 1813 dry year, whereas the disturbed trees show lasting reduced growth beginning in 1813.

cent adobe church continued in service for the rest of the century (*17*) and is still standing today. The lack of reported aftershocks at San Juan Capistrano (*18*) also implies a distant source, as does the lack of damage at San Luis Rey (*3*). The second argument is also unconvincing because the record of events in the early 1800s is meager, even for coastal missions. There were Indian settlements (rancherias) and private ranchos in the region between San Bernardino and San Gabriel, but there are no written records from them today (*18, 20*).

Because fault slippage apparently caused the trauma evidenced by the nine conifers, we conclude that 12 km (the linear distribution of the nine disturbed trees) is the minimum surface rupture length associated with the 8 December 1812 earthquake. Empirical data from California strike-slip earthquakes suggest that such an earthquake would have been M_W ~6.0 (*21*).

Other evidence suggests that the earthquake was larger. Slippage associated with such a small event is typically only a few centimeters to decimeters—too little to shear major tree roots or damage crowns. Moreover, the 22 July 1899 earthquake (M_W = 6.5), which originated near Wrightwood, was less intense at San Gabriel than was the 1812 event. For these reasons, a rupture length greater than 12 km and a $M_W \geq 6.5$ are likely.

The last prehistoric earthquake recorded at Pallett Creek (Fig. 1) (*1, 2, 4*) may be the same event that is recorded by the disturbed trees. New, precise radiocarbon analyses date the Pallett Creek event at A.D. 1785 ± 32, which includes 1812. If this correlation is correct, then the 8 December 1812 quake ruptured at least 27 km and would have had a $M_W \geq 7.0$. The vertical and strike-slip deformation associated with this event at Pallett Creek, about 6 m (*22*), is similar to that produced during the 1857 earthquake, which ruptured 360 km. Thus, we estimate that the 8 December 1812 rupture segment was at least fifty and perhaps hundreds of kilometers.

Paleoseismic data from three other sites limit the length of the 8 December 1812 rupture segment. (i) Near Indio and Salton Sea (Fig. 3), the San Andreas fault has right-laterally slipped only about 1.1 m since A.D. 1680; this amount has been attributed to aseismic creep (*23*). (ii) On the basis of ^{14}C dates, the most recent fault rupture at Lost Swamp occurred before the early 19th century (*24*); however, the possibility that this event was the 1812 earthquake and the ^{14}C dates are in error cannot be completely ruled out. (iii) Liquefaction and faulting at Mil Potrero that was ^{14}C-dated to A.D. 1760 ± 100 might also be evidence of the

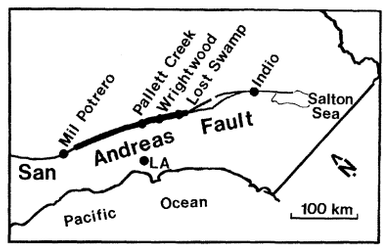

Fig. 3. Map of the estimated 8 December 1812 earthquake rupture segment (thick line), on the basis of all dendrochronologic, paleoseismic, and historical evidence.

1812 earthquake (*25*). This interpretation is confounded, however, by tree-ring evidence from a Jeffrey pine growing 3 m from the fault near Mil Potrero. Despite being about 1.5 m in diameter in 1812, this tree was not disturbed then. It was, however, greatly affected by the 1857 earthquake (*8*).

On the basis of dendrochronologic, paleoseismic, and historical evidence, we conclude that the San Andreas fault northeast of Los Angeles ruptured in 1812, only 44 years before the great 1857 earthquake. We place its southeastern terminus at Lost Swamp and its northwestern terminus just southeast of Mil Potrero (Fig. 3); this is a total length of about 170 km, which is consistent with several meters of offset at Pallett Creek.

The period of fault dormancy before 1812 was about 330 years (*4*), which indicates that recurrence intervals for this part of the San Andreas fault do not cluster tightly around the 131-year average. This erratic behavior may have been caused by nonuniform stress accumulation; perhaps stress accumulated along the fault more slowly from 1480 to 1812 than from 1812 to 1857. Another possible explanation is that large earthquakes do not relieve all of the stress on faults. Perhaps the 1812 event relieved only part of the stress accumulated between 1480 and 1812, and then the remaining stress was relieved in 1857. Regardless of the explanation, the remarkable variability of intervals between the latest three large earthquakes on the San Andreas fault near Los Angeles indicates that a more fundamental knowledge of fault dynamics is critical for accurate prediction of future destructive earthquakes.

REFERENCES AND NOTES

1. K. E. Sieh, *J. Geophys. Res.* **83**, 3907 (1978).
2. ———, *ibid.* **89**, 7641 (1984).
3. D. Agnew and K. E. Sieh, *Bull. Seismol. Soc. Am.* **68**, 1717 (1978).
4. On the basis of the paleoseismic record at Pallett Creek (Fig. 1) (K. Sieh, M. Stuiver, D. Brillinger, in preparation).
5. For example, A. C. Lawson *et al.*, *Carnegie Inst. Washington Publ. 87* (1908), p. 64; M. L. Fuller, *U.S. Geol. Surv. Bull. 494* (1912), pp. 95–99; G. D. Louderback, *Bull. Seismol. Soc. Am.* **37**, 37 (1947),

p. 57; G. Plafker, in *The Great Alaska Earthquake of 1964* (National Research Council, National Academy of Sciences, Washington, DC, 1972).
6. H. O. Wood and F. Neumann, *Bull. Seismol. Soc. Am.* **21**, 277 (1931).
7. R. Page, *Geol. Soc. Am. Bull.* **81**, 3085 (1970); R. E. Wallace and V. C. LaMarche, *Earthquake Inf. Bull.* **2**, 127 (1979); G. C. Jacoby and L. D. Ulan, *J. Geophys. Res.* **88**, 9305 (1983).
8. K. E. Meisling and K. E. Sieh, *J. Geophys. Res.* **85**, 3225 (1980).
9. P. R. Sheppard and G. C. Jacoby, in preparation.
10. M. A. Stokes and T. L. Smiley, *An Introduction to Tree-Ring Dating* (Univ. of Chicago Press, Chicago, 1968); M. G. L. Baillie and J. R. Pilcher, *Tree-Ring Bull.* **33**, 7 (1973). All cross-dating was rechecked with a reiterative comparison procedure [R. L. Holmes, *Tree-Ring Bull.* **43**, 69 (1983)].
11. L. D. Drew, Ed., *Tree-Ring Chronologies of Western America, III: California and Nevada* (Chronology Series 1, Univ. of Arizona Press, Tucson, 1985).
12. G. C. Jacoby, *Tree Ring Soc. News.* **21**, 4 (1982).
13. Trees typically do not produce annual growth rings in the lower trunk when severely stressed or disturbed because lower-stem wood production is a low priority function compared to bud, shoot, and root growth [J. C. Gordon and P. R. Larson, *Plant Physiol.* **43**, 1617 (1968)].
14. E. R. Cook, thesis, University of Arizona, Tucson (1985); D. A. Graybill, in *Climate from Tree Rings*, M. K. Hughes, P. M. Kelly, J. R. Pilcher, V. C. LaMarche, Eds. (Cambridge Univ. Press, Cambridge, 1982), pp. 21–28.
15. In White Fir 1, the 1857 earthquake trauma was greater than that of 1812 to 1813 (Fig. 2).
16. On the basis of the annual growth cycle of Jeffrey pine in this area as determined from our own collections.
17. T. R. Toppozada, C. R. Real, D. L. Parke, *Calif. Div. Mines Geol. Open-File Rep. 82-11 SAC* (1982).
18. H. H. Bancroft, in *History of California* (Bancroft, San Francisco, 1885), vol. II, 1801 to 1824.
19. Fr. Engelhardt, Z., *San Juan Capistrano Mission* (Standard Printing Company, Los Angeles, 1922).
20. G. W. Beattie and H. P. Beattie, *Heritage of the Valley* (Biobooks, Oakland, CA, 1951), pp. 5–17.
21. D. B. Slemmons, *U.S. Army Miscellaneous Paper S-73-1* (Report to Office, Chief of Engineers, U.S. Army, Washington, DC, 1977).
22. S. Salyards, K. E. Sieh, J. Kirschvink, in preparation.
23. K. E. Sieh, *Eos* **67**, 1200 (1986); P. L. Williams and K. E. Sieh, *ibid.* **68**, 1506 (1987).
24. R. Weldon II and K. E. Sieh, *Geol. Soc. Am. Bull.* **96**, 793 (1985).
25. T. L. Davis, thesis, University of California, Santa Barbara (1983). Davis reported a 1σ error of ±50; we use a 2σ error of ±100.
26. We thank L. R. Sykes and E. R. Cook for reviews and L. O. White for field assistance. This work was supported by NSF grants EAR 85-19030 and EAR 87-07967 and U.S. Geological Survey grant 14-08-0001-G1329 to G.C.J. and P.R.S. and U.S. Geological Survey grants 14-08-001-G1098 and G1370 to K.E.S. Lamont-Doherty Geological Observatory contribution No. 4326; California Institute of Technology Geological and Planetary Sciences Contribution No. 4644.

16 March 1988; accepted 31 May 1988

Isolation and Characterization of a Novel Protein (X-ORF Product) from SIV and HIV-2

L. E. HENDERSON, R. C. SOWDER, T. D COPELAND, R. E. BENVENISTE, S. OROSZLAN

A protein designated p14 was purified from a simian immunodeficiency virus (SIV_{Mne}) and was shown by amino acid sequence analysis to be nearly identical to the predicted translational product of a unique open reading frame (X-ORF) in the nucleotide sequences of SIV_{mac} and human immunodeficiency virus type 2 (HIV-2). Thus the X-ORF is proven to be a new retroviral gene. The p14 is present in SIV_{Mne} in molar amounts equivalent to those of the *gag* proteins. This is the first example of a retrovirus that contains a substantial quantity of a viral protein that is not a product of the *gag*, *pro*, *pol*, or *env* genes. SIV p14 and its homolog in HIV-2 may function as nucleic acid binding proteins since purified p14 binds to single-stranded nucleic acids in vitro. Antisera to the purified protein detected p14 in SIV_{Mne}, SIV_{mac}, and a homologous protein (16 kilodaltons) in HIV-2 but did not react with HIV-1. Diagnostic procedures based on this novel protein will distinguish between HIV-1 and HIV-2.

SIMIAN IMMUNODEFICIENCY VIRUSES (SIVs) cause a fatal disease (in susceptible primate species) with symptoms (*1, 2*) similar to those associated with human AIDS, which is caused by human immunodeficiency viruses type 1 (HIV-1) and type 2 (HIV-2). Strains of SIV were originally isolated from rhesus monkeys (*Macaca mulatta*) with immunodeficiency or lymphoma (SIV_{mac}) (*3*), and subsequently from asymptomatic mangabey monkeys (SIV_{SMM}, SIV_{SMLV}, and SIV_{Delta}) (*4*), and from a *Macaca nemestrina* with lymphoma (SIV_{Mne}) (*5*). A strain of SIV originally thought to be obtained from African green monkeys ($STLV\text{-}III_{agm}$) (*6*) has since been shown to be SIV_{mac} (*7*). SIV strains are closely related to each other (greater than 90% identity) (*8, 9*) and also partially related to HIV-1 (40% nucleotide sequence identity) but are more closely related to HIV-2 (75% overall nucleotide sequence identity) (*8*).

The genomic organizations of HIV-1 (*10*), HIV-2 (*11*), and SIV (*8*) are very similar; each contains open reading frames (ORFs) designated *gag*, *pol*, *env*, Q, R, trs, tat, and F. However, HIV-2 and SIV contain an ORF designated X that is not found in HIV-1 (*8, 11*). The X-ORF is located in the central region of the genome between the *pol*-ORF and the *env*-ORF. Here we report the isolation and molecular characterization of a protein from SIV_{Mne} designated p14 and show by amino acid sequence analysis that it is the product of the X-ORF.

A single-cell clone of Hut-78 cells infected with SIV_{Mne} (clone E11S) was grown, and virus was purified by sucrose density gradient centrifugation (*5*). Viral proteins were purified by reversed-phase high-pressure liquid chromatography (RP-HPLC) and characterized by NH_2- and COOH-terminal amino acid sequence analysis (*12*). Our earlier analysis showed that SIV_{Mne} proteins designated p28, p16, p8, p6, p2, and p1 were proteolytic cleavage products of the viral *gag* precursor ($Pr60^{gag}$), which has the following complete structure: p16-p28-p2-p8-p1-p6 (*9*). We also reported a protein (designated p14) (*5*) that did not appear to be a *gag* protein (*9*) but was of viral origin since macaques infected with SIV_{Mne} raised readily detectable antibodies to the protein (*2, 9*).

Partially purified SIV_{Mne} p14 (*9*) was rechromatographed by RP-HPLC to give a homogeneous preparation as shown by SDS–polyacrylamide gel electrophoresis (PAGE) analysis (Fig. 1A, lane 2). Purified p14 was inert to Edman degradation (gas-phase sequencer), which suggested that it had a derivatized NH_2-terminal residue (blocked NH_2-terminus). To obtain amino acid sequence information for identification of p14, we digested the protein with trypsin and purified peptides (Fig. 2A, a to l) for analysis to determine amino acid compositions and sequences. The determined amino acid sequences and compositions were compared with the translated proviral DNA sequence of SIV_{mac} (*8*) and HIV-2 (*11*) and found to be highly homologous to predicted sequences located in the X-ORF of each virus. The SIV_{Mne} p14 peptides (Fig. 2B) align with residues predicted by the X-ORF of HIV-2 starting at position 2 and continue through position 112 except that peptides corresponding to predicted residues 69 through 70 and 85 through 88 were not isolated. Of the 105 amino acid residues of SIV_{Mne} p14 that were determined by analysis

L. E. Henderson, R. C. Sowder, T. D. Copeland, S. Oroszlan, Laboratory of Molecular Virology and Carcinogenesis, Bionetics Research, Inc. (BRI)–Basic Research Program, National Cancer Institute, Frederick Cancer Research Facility, Frederick, MD 21701.
R. E. Benveniste, Laboratory of Viral Carcinogenesis, National Cancer Institute, Frederick, MD 21701.